Computer Vision

Matteo Galiazzo

April 8, 2025

Contents

1 Introduction

The difference between computer vision and image processing is the fact that computer vision is the process of extracting information from images, while image processing aims at improving the quality of images. Quite often image processing helps computer vision. The informations we want to extract from the images could be counting, object orientation, object classification, measurements... Computer vision is challenging since we lose depth from the images (3D information becomes 2D), scale and illumination varies, and there's object occlusion (object hiding other objects).

Computer vision started with hand-crafted decision rules that only required few images as example, and evolved to machine learning where the algorithm learns a decision rule, but the training requires hundreds to thousands of images. The big paradigm shift happened with deep learning (e2e learning) which learned both the image representation and the decision rules, but required thousands to millions of words. Deep learning has been enabled by better networks, better hardware and more data.

2 Fundamentals of Image Processing and Computer Vision

2.1 Images

An imaging device gathers the light reflected by 3D objects to create a 2D representation of the scene.

2.1.1 Pinhole camera model

The "pinhole camera" is the simplest camera model we can define. Light goes through the very small pinhole (to not have saturation) and hits the image plane. Geometrically, the image is achieved by drawing straight rays from scene points through the hold up to the image plane.

This simple geometrical model turns out to be a good approximation of the geometry of image formation. However, useful images can hardly be captured by means of a pinhole camera.

The **geometric model of image formation** in a pinhole camera is known as **perspective projection**.

M : scene point
m : corresponding image point
I : image plane
C : optical centre (pin hole)
Optical axis: line through C and orthogonal to I
c : intersection between optical axis and image plane (image centre or piercing point)
f : focal length
F : focal plane

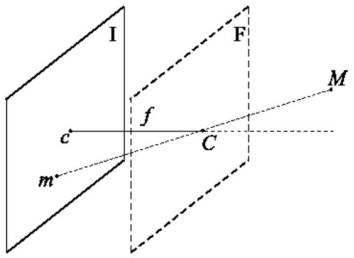

Figure 1: perspective projection

Which, by writing the poitns as vectors and the plane's coordinates, becomes the geometric model in the image 2

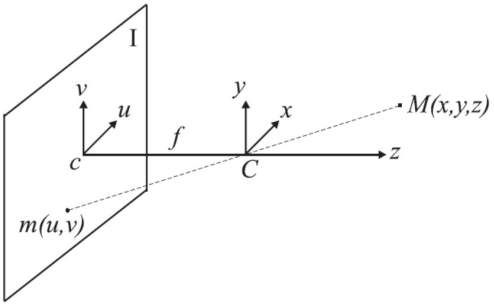

Figure 2: geometric model of image formation

Given the reference frame in the image 2

- u is the horizontal axis in the image plane.
- v is the vertical axis in the image plane.
- X and Y are the respective axis in the 3D reference system. It's called the **camera reference system** because it is "attached" to the camera.

For the perspective model these axis must be parallel

The equations to map scene points into their corresponding image points are defined as:

$$\frac{u}{x} = -\frac{f}{z} \rightarrow u = -x\frac{f}{z} \qquad \frac{v}{y} = -\frac{f}{z} \rightarrow v = -y\frac{f}{z}$$

The minus sign means the axis gets inverted (as we can see in the visualization, and it's what happens in the brain). We can get rid of the sign, since the image plane can be though of as lying in front rather than behind the optical centre.

Image coordinates are a scaled version of scene coordinates (function of depth). When z increases, since it's at the denominator in both the equations, the terms gets smaller (object gets smaller in the image). When f increases, since it's at the numerator in both the equations the term gets bigger (object gets bigger in the image)

As we previously said, the image formation process deals with mapping a 3D space onto a 2D space, and so to the loss of depth information. A given scene point is mapped into an image point, but an image point is mapped onto a 3D line. For an image point we can only state that its corresponding scene point lays on a line, but cannot disambiguate a specific 3D point along the line.

2.1.2 Stereo images

We use multiple images to create stereo vision. Given correspondences, 3D information can be recovered easily by triangulation. We can use two cameras, or two cameras and an infrared sensor to project guides to align the images.

For standard stereo geometry there are some assumptions we have to make:

- The cameras have parallel (x, y, z) axes.
- The image planes of both cameras are coplanar and aligned.
- Both cameras have identical focal lengths.

Based on this, the transformation between the two reference frames is just a translation, usually horizontal. For stereo vision is also really important to **sense two images at the same moment**.

The cameras are displaced at a given quantity b called baseline. The **disparity** is the difference between the horizontal coordinates in the left and right images.

In standard stereo geometry since we are given just two 2D images there is no info about the correspondence between two points in the two images. We can recall that the camera have parallel axes, and so we know that we can search for the correspondence along the horizontal lines. This task is called stereo matching.

2.1.3 Stereo correspondence

In stereo correspondence, given a point in one image, we have to find it in the other image which is the projection of the same 3D point. Such image points are called corresponding points. **Points**

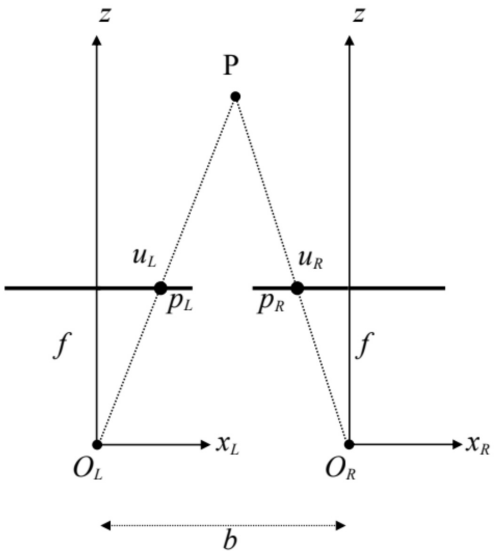

Figure 3: standard stereo geometry

farther away have a smaller disparity, while close points have a larger display.

Figure 4: Corresponding points look similar in the two images

The image of a 3D line segment of length L lying in a plane parallel to the image plane at distance z from the optical centre will exhibit a length given by:

$$l = L\frac{f}{z}$$

This relationship is more complicated for an arbitrarily oriented 3D segment, as its position and orientation need to be accounted for as well. For a **given position and orientation, length always shrinks alongside distance**.

Perspective projection maps 3D lines into image lines. **Parallelism between 3D lines is not preserved** (except for lines parallel to the image plane). This is the reason why if we look at a really long road into the distance we have the perception that the road becomes thinner, and the lines of the road intersect in the distance. The images of parallel 3D lines intersect at a point, called **vanishing point**, which isn't necessarily within the image.

If the lines are parallel to the image plane they meet at infinity.

2.1.4 Epipolar geometry

What if the two cameras are no longer aligned? Do we need to search through the whole image? We can project the line related to point P_L in the right plane and search across that line. The

issue is that this projection can be computed only if the transformation between the two cameras is known (the relative mapping between the two cameras).

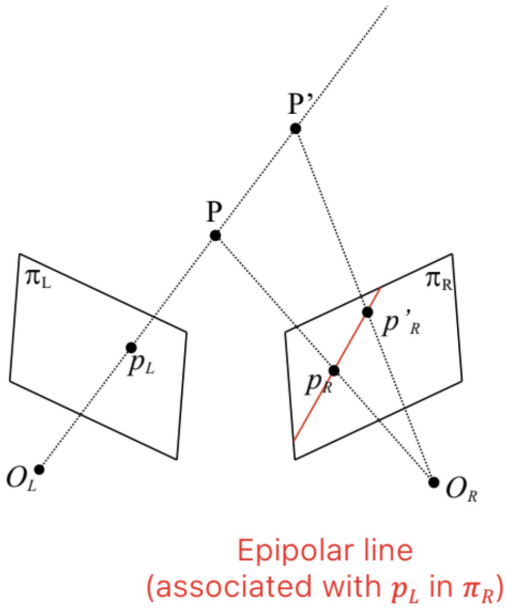

Figure 5: Epipolar line

It is almost impossible to build a stereo rig which is perfectly aligned horizontally. Searching through oblique epipolar lines is awkward, and computationally is less efficient. What people do in practice is to convert epipolar geometry to standard geometry with rectification/warping. We warp the images as if they were acquired through a standard geometry, then we can compute and apply to both images a transformation known as rectification.

2.1.5 Depth of Field (DOF)

A scene point is on focus when all its light rays, gathered by the camera, hit the image plane at the same point. In a pinhole device this happens to all scene points because of the very small size of the hole, so that the camera features an infinite Depth of Field (DOF).

The drawback is that such a small aperture allows gathering a very limited amount of light. The image is really sharp, but has a really low light. If a point is projected onto a circle instead of a point (bigger pinhole) the image is not sharp (not on focus). If we cannot gather enough light through the aperture we have to integrate through time, by using a longer exposure time.

2.1.6 Lenses

Lenses concentrate light, so we use them to gather more light from a scene point and focus it on a single image point. This enables much smaller exposure times. This way Depth Of Field is no longer infinite, and only a limited range of points can be simultaneously on focus in a given image.

We will consider the approximate model known as thin lens equation, which is useful to graphically determine the position of a focused image point:

- Rays parallel to the optical axis are deflected to pass through F.
- Rays through C are undeflected.

If the image is on focus, the image formation process obeys to the perspective projection model:

- The center of the lens is the optical center.
- The distance v acts as the effective focal length of the projection.

Choosing the distance of the image plane determines the distance at which scene points appear on focus in the image. Scene points in front and behind the focusing plane will result out-of-focus, thereby appearing in the image as **blur circles**, rather than points.

The advantage of lenses is to have a small exposure time for capturing moving objects but we pay in terms of Depth Of Field.

As we can see in 2.1.6 having a small aperture (pinhole camera model) results in everything being on focus, but we need lots of light, or the image will be dark, since few light can enter in

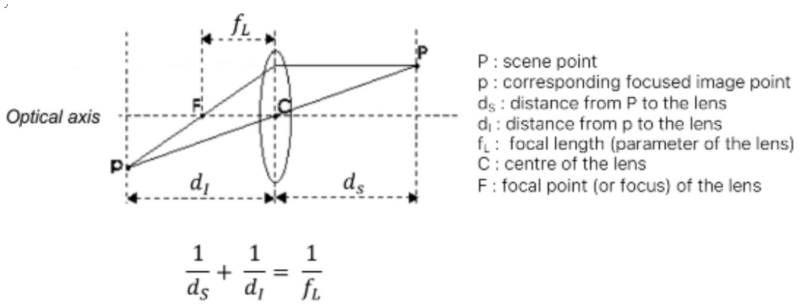

Figure 6: Scheme of a lens

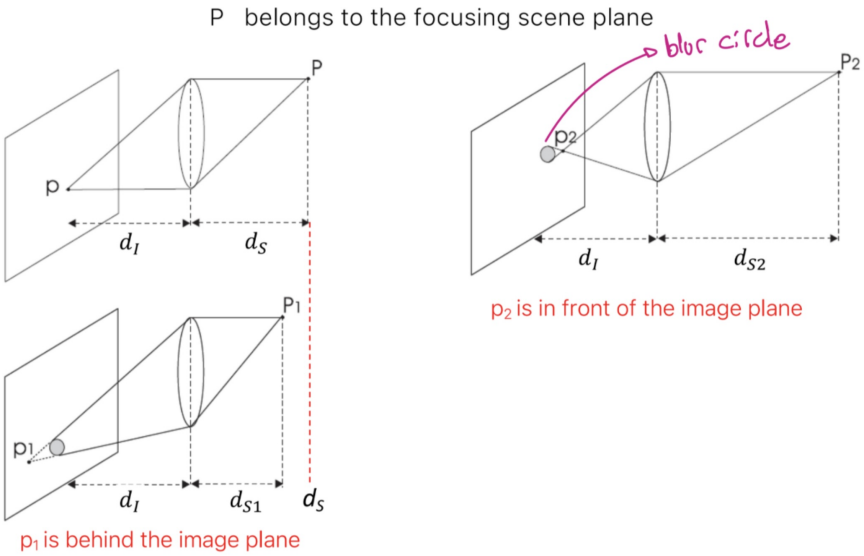

Figure 7: Lens focusing at various distances

the sensor. We could also increase our exposure time to let more light in, but in that case we need the objects in our image to be still. Having a bigger aperture results in more light coming in in a small time fraction, but the lens distortion causes the light to be focused only at certain distances, and creates blur cirlces in other zones, so we get a lower depth of field, as we can see in 7.

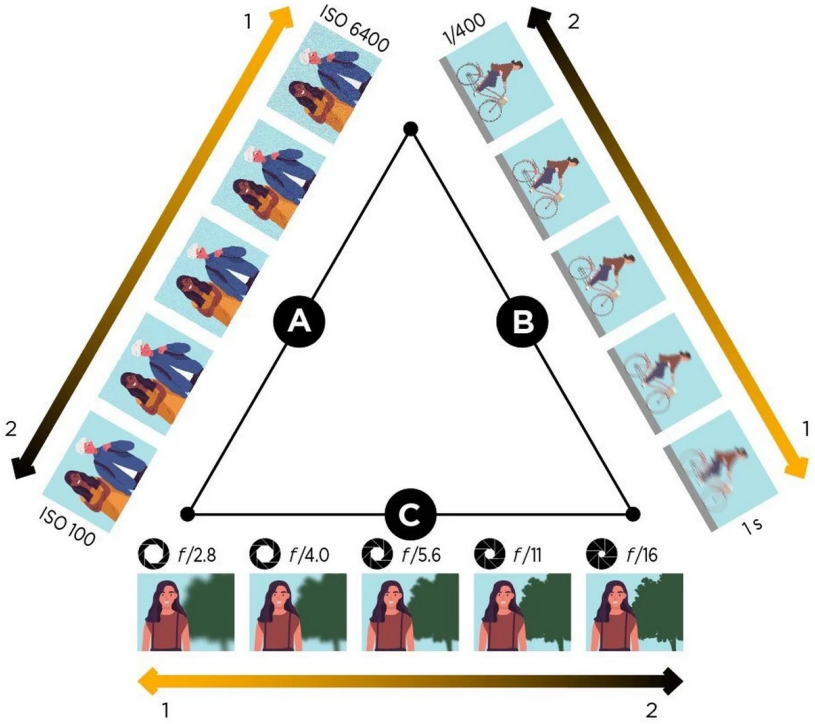

2.1.7 Diaphragm

In theory, when imaging a scene through a thin lens, only the points at a certain distance can be on focus, all the others appear blurred into circles. However, as long as the circles are smaller than the size of the photosensing elements (a single pixel), the image will still look on-focus.

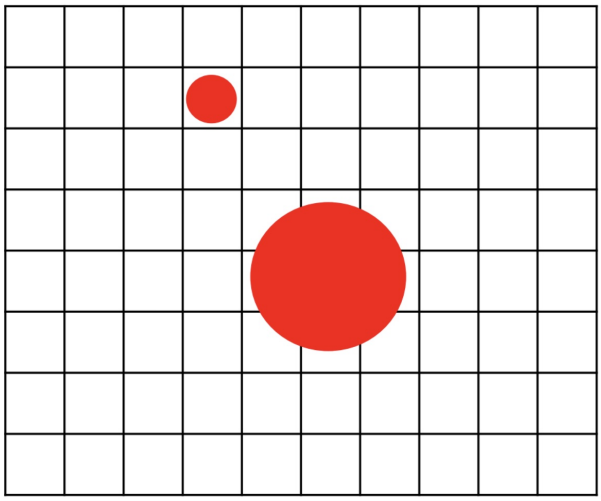

Figure 8: Blurring at pixel level

The range of distances across which the image appears on focus, due to blur circles being small enough, determines the (Depth Of Field) of the imaging apparatus. Cameras often deploy an adjustable diaphragm (iris) to control the amount of light gathered through the effective aperture of the lens.

- Reduce aperture → less light → smaller blur circle
- More aperture → more light → larger blur circle.
- Close the diaphragm → increase depth of field → not enough light → increase exposure time → moving object → motion blur.

2.1.8 Focusing mechanism (manually changing depth of field)

To focus on objects at diverse distances we need a mechanism that allows the lens (or the lens subsystem) to translate along the optical axis with respect to the fixed position of the image plane.

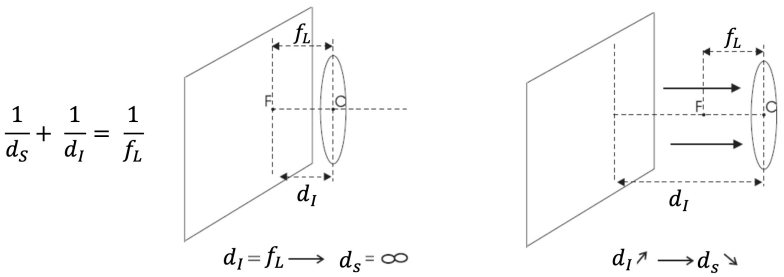

Figure 9: Focusing mechanism

At one end position ($d_I = f_L$) the camera is focused at infinity (objects at inifity are on sharp focus). The focusing mechanism allows the lens to be translated farther away from the image plane up to a certain maximum value, which determines the minimum focusing distance.

2.1.9 Image digitization

How do we convert a continuous image to a discrete one which can be represented on a computer? The process can be divided in two steps: sampling and quanitzation.

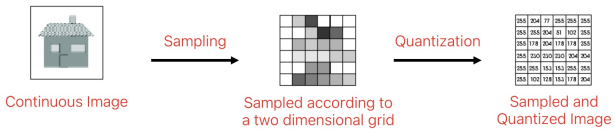

Figure 10: The two steps of the image digitization process

- **Sampling**: the planar continuous image is sampled along both the horizontal and vertical directions to pick up a matrix of $N \times M$ samples (pixels).
- **Quantization**: the continuous range of values associated with pixels is quantized into $l = 2^m$ discrete levels known as gray-levels. m is the number of bits used to represent a pixel, with the memory occupancy (in bits) of a gray-scale image given by $B = N \times M \times m$. Coloured digital images are typically represented within computers using 3 bytes per pixels. Both more pixels and more bits per pixel result in a higher quality image.

The more bits we spend for its representation, the higher the quality of the digital image (it becomes a closer approximation to the ideal continuous image). This applies both to sampling and quantization.

2.1.10 Camera sensors

The sensor is a matrix of photodetectors. During exposure time, each detector converts the incident light into a proportional electic charge. The companion circuitry reads-out the charge to generate the output signal, which can be either digital or analog. For digital cameras the sensor includes the necessary ADC circuitry.

Today, the two main sensor technologies are:

- **Charge Coupled Devices (CCD)**, where the sensor and circuit are separated.
- **Complementary Metal Oxide Semiconductor (CMOS)**, where everything is on the same circuit.

CCD/CMOS sensors can't sense colors, so we place an array of optical filters in front of the photodetectors, to render each pixel sensitive to a specific range of wavelengths.

2.1.11 SNR

The intensity measured at a pixel under perfectly static conditions varies due to the presence of random noise. The main noise sources are:

- **Photon Shot Noise**: the number of photons collected during exposure time is not constant.
- **Electronic Circuitry Noise**: generated by the electronics.
- **Quantization Noise**: related to the ADC conversion.
- **Thermal Noise (Dark Current Noise)**: random charge observed due to thermal excitement.

SNR can be expressed both in decibels and bits.

2.1.12 Dynamic Range (DR)

If the sensed amount of light is too small, the "true" signal cannot be distinguished from noise. Given $E_{\min}$: the minimum detectable irradiation, and $E_{\max}$, the saturation irradiation. The Dynamic Range (DR) of a sensor is defined as $DR = \frac{E_{\max}}{E_{\min}}$, and like the SNR, it is often specified in decibels or bits.

Like SNR, the higher the DR the better it is. A **higher DR** corresponds to the ability of the sensor to simultaneously **capture in one image both the dark and bright** structures of the scene.

2.2 Image Filtering

2.2.1 Noise and image filters

In computer vision we have to deal with noise. Noise is always different, and more noticeable in uniform regions of the image. The simplest thing to reduce noise is to output the average of the pixel color over time, to get **almost** the ideal noiseless value.

$$O(p) = \frac{1}{T}\sum_{t=1}^{T} I_k(p) = \frac{1}{T}\sum_{t=1}^{T}(\tilde{I}(p) + n_t(p))$$

This technique works well on still images.

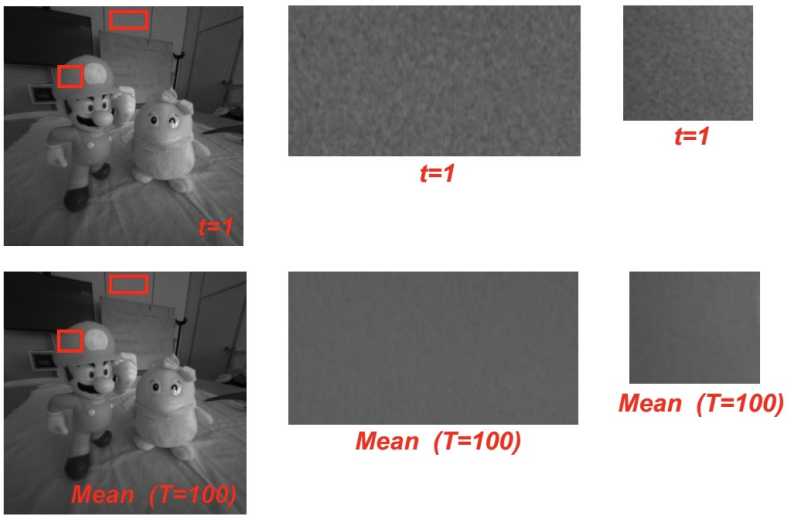

Figure 11: Simple denoising

If we are given a simple image, we may compute a mean across neighbouring pixels, like a spatial rather than temporal mean. The size of the square of the neighbouring pixels is a tradeoff.

This is a very basic denoising filter.

Image filters are image processing operators that compute the new intensity (colour) of a pixel, p, based on the intensities (colours) of those belonging to a neighbourhood (support) of p.

2.2.2 Convolution

An important sub-class of filters is given by **Linear** and **Translation-Equivariant (LTE)** operators.

The **application of filters** in image processing consists in a **2D convolution** between the input image and the impulse response function of the LTE operator.

LTE operators are used as feature extractors in Convolutional Neural Networks (CNNs).

Given an input 2D signal $i(x, y)$, a 2D operator $Ti(x, y)$ is said to be linear if and only if

$$T\{\alpha i_1(x, y) + \beta i_2(x, y)\} = \alpha o_1(x, y) + \beta o_2(x, y)$$

with $o_1 = Ti_1$ and $o_2 = Ti_2$ and α, β are two constants. The operator is said to be **translation-equivariant** if and only if: $T\{i(x - x_0, y - y_0)\} = o(x - x_0, y - y_0)$

If the operator is LTE, the output signal is given by the **convolution** between the input signal and the impulse response (point spread function) $h(x, y) = T\delta(x, y)$.

$$o(x, y) = i(x, y) * h(x, y) = T\{i(x, y)\}$$

$$i(x, y) * h(x, y) = \int_{-\infty}^{\infty} \int_{-\infty}^{\infty} i(\alpha, \beta) h(x - \alpha, y - \beta)\, d\alpha d\beta$$

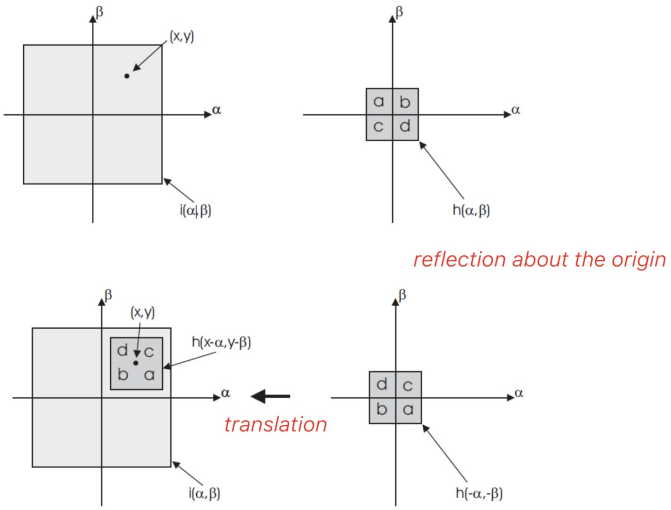

Figure 12: A graphical view of convolution

Convolutions have some useful properties:

- **Associative property**: $f * (g * h) = (f * g) * h$ (useful because we can decompose kernels and obtain faster operations).
- **Commutative property**: $f * g = g * f$.
- **Distributive property**: $f * (g + h) = f * g + f * h$.
- **Convolution commutes with differentiation**: $(f * g)' = f' * g = f * g'$.

The correlation of signal $i(x, y)$ with respect to signal $h(x, y)$ is defined as:

$$i(x, y) \circ h(x, y) = \int_{-\infty}^{\infty} \int_{-\infty}^{\infty} i(\alpha, \beta) h(x - \alpha, y - \beta)\, d\alpha d\beta$$

Correlation is not commutative, unlike the convolution.

2.2.3 Discrete convolution

Normal convolution is useful for signal theory, but we want to have a discrete convolution, where we use summations instead of integrals. The four convolution properties highlighted for the convolution hold for the discrete one too.

2.2.4 Practical implementation

CNNs learn flipped kernels. In image processing both the the input image and the kernel are stored into matrices of given finite sizes, with the image being much larger than the kernel. Conceptually, to obtain the output image we need to slide the kernel across the whole input image and compute the convolution at each pixel.

We have an issue on borders, since the kernel "goes out" of the matrix of the image. We have two main options to solve this issue:

- `CROP`: common in image processing.
- `PAD`: preferred in CNNs. We can do zero-padding, replicate the first pixel many times, reflect the first k pixels (half of the kernel)...

Without padding convolutions shrink the images.

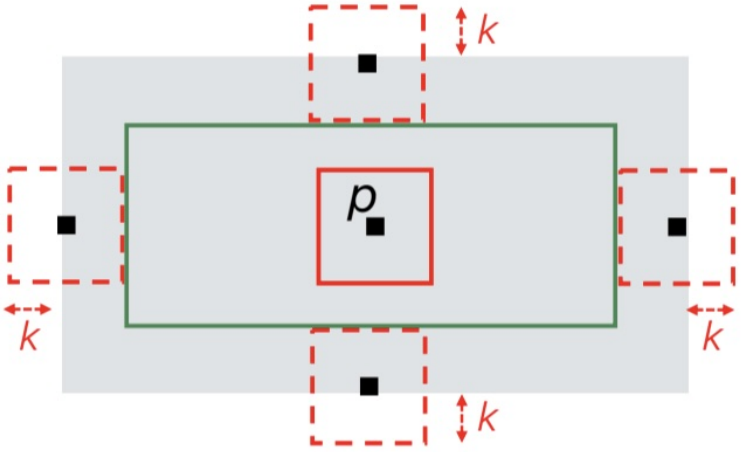

Figure 13: Issues with convolutions

2.2.5 Mean filter

Mean filtering is the **simplest and fastest way to denoise an image**. It consists in replacing each pixel intensity by the average intensity overa chosen neighbourhood. According to signal processing theory, **the Mean Filter carries out a low-pass filtering operation**, which in image processing is **also referred to as image smoothing**. Smoothing is often aimed at image denoising, but sometimes is used to cancel out small-size unwanted details that might hinder the image analysis task. Linear filtering **reduces noise but blurs the image**, so we lose sharpness.

2.2.6 Gaussian filter

The Gaussian filter is an LTE operator whose impulse response is a 2D Gaussian function.

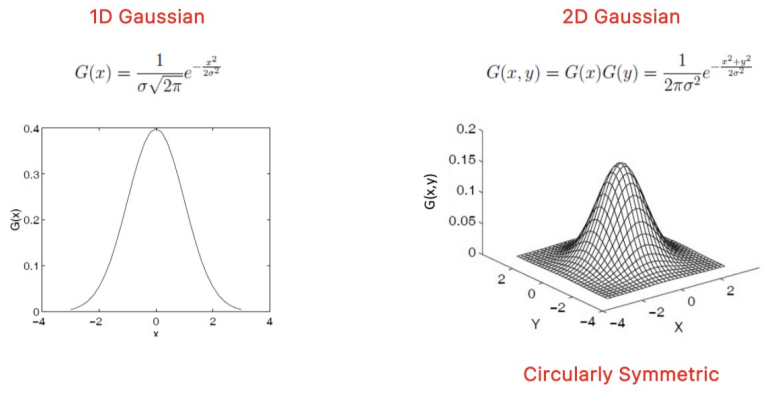

Figure 14: 1D and 2D Gaussian plot

The larger the size of the gaussian kernel, the more accurate the approximation will be, but the computational cost grows with the filter size. We should then use larger sizes for filters with

higher σ, smaller sizes whenever σ is smaller. A typical rule is to choose the size of the filter by capturing the interval $[-3\sigma, +3\sigma]$ since it captures 99% of the energy of the Gaussian impulse. To speedup the filtering we can apply the 2D gaussian by doing 2 1D gaussian filterings.

We also observe that the higher the σ, the higher is the smoothing caused by the filter. We can use this filter to remove details from the image.

2.2.7 Median filter

There is noise that Gaussian filters can't handle well, that is the salt and pepper noise. It's usually caused by image corruption (or broken pixels in the sensor). Linear filtering is ineffective and just blurs the image.

We can use a **non-linear filter**, where each pixel intensity is replaced by the **median over a given neighbourhood**. Median filtering counteracts impulse noise effectively, since **outliers tend to fall at either the top or the bottom end of the sorted intensities**. Median filtering tends to keep sharper edges than linear filters such as the Mean or the Gaussian.

Figure 15: Example of the power of the median filter

The median filter can effectively denoise the image without introducing significant blur, yet, Gaussian-like noise, such as sensor noise, cannot be dealt with by the median, as this would require computing new noiseless intensities.

2.2.8 Bilateral filter

The bilateral filter preserves edges while filtering out noise. It's an advanced non-linear filter to accomplish **denoising of Gaussian-like noise without blurring the image**. It's also called edge preserving smoothing.

$$O(p) = \sum_{q \in S} H(p,q) \cdot I_q \qquad H(p,q) = \frac{1}{W(p)} G_{\sigma_s}(d_s(p,q)) G_{\sigma_r}(d_r(p,q))$$

- **spatial distance**: $d_s(p,q) = ||p-q||_2 = \sqrt{(u_p - u_q)^2 + (v_p - v_q)^2}$.
- **range (intensity) distance**: $d_r(I_p, I_q) = |I_p - I_q|$.
- **normalization factor**: $W(p) = \sum_{q \in S} G_{\sigma_s}(d_s(p,q)) G_{\sigma_r}(d_r(p,q))$

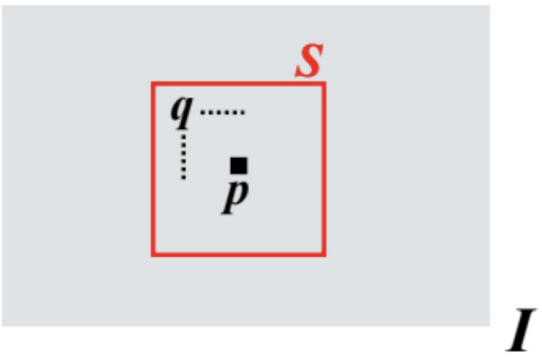

Figure 16: Application of the bilateral filter

Given the supporting neighbourhood, neighbouring pixels take a larger weight as they are both closer and more similar to the central pixel. At a pixel nearby an edge, the neighbourhood falling

on the oter side of the edge looks quite different and thus cannot contribute significantly to the output value due to their weights being small. **The kernel has to be recomputed for each pixel**.

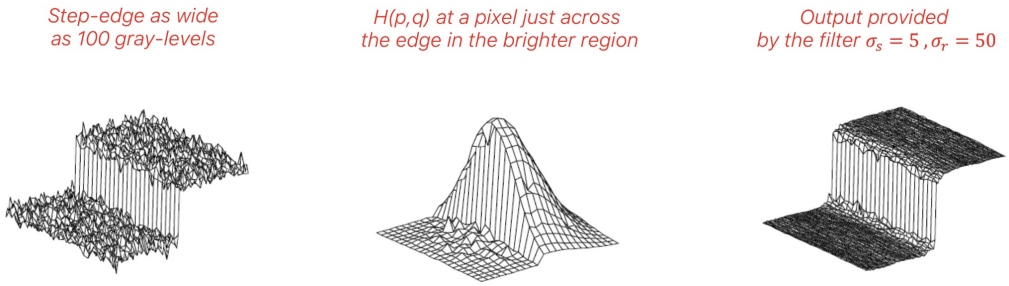

Figure 17: Bilateral filter differences

2.2.9 Non-local means filter

It's another non-linear edge preserving smoothing filter. The key idea is that the **similarity among patches spread over the image** can be deployed to achieve denoising. It's even more expensive than the bilateral filter, since it has to look at more of the image.

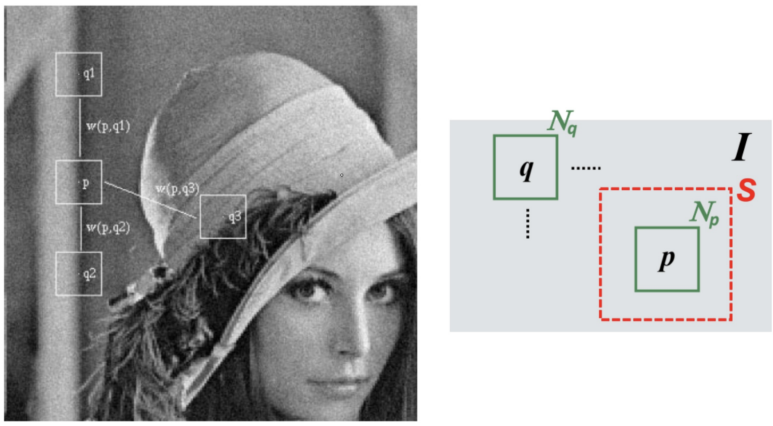

Figure 18: Non-local means filter

Figure 19: Difference between Gaussian filter and non-local means filter

2.3 Edge detection

Edge points are local features of the image that capture important information related to its semantic content. Edges are pixels that lie exactly in between image regions of different intensities.

1D step-edge We can detect an edge with a sharp change of a 1D signal (1D step-edge). The simplest edge-detection operator relies on thresholding the absolute value of the derivative of the signal.

2D step-edge A 2D step-edge is characterized not only by its strength but also by its direction (diagonal edge). The operator which allows us to sense the edge in any direction is the gradient:

$$\nabla I(x,y) = \frac{\partial I(x,y)}{\partial x} i + \frac{\partial I(x,y)}{\partial y} j$$

The **gradient tells the direction along which the function exhibits its maximum variation**. We can use differences to approximate the gradient (since we are in the discrete world and we talk about pixels, not functions). We can estimate the magnitude of the gradient by using different approximations. We choose $|\nabla I|_{\max} = \max(|I_x|, |I_y|)$, since it's fast and invariant with respect to the edge direction.

Edges and noise In real images an edge will not look as smooth as we have seen due to noise. Taking derivatives of noisy signals is an ill posed problem (the solution is not robust with respect to the input variation) since derivatives amplify noise. Noise robustness is usually achieved by smoothing the signal before computing the derivatives required to highlight edges. Smoothing has the side effect of blurring true edges, making it more difficult to detect and localize them, since pixel of different colors will look similar after filtering because of the blending.

Prewitt and Sobel Prewitt and Sobel address the challenge of detecting edges in noisy environments by combining smoothing and differentiation into a single step. The Prewitt and Sobel operators perform spatial filtering by using 3×3 convolution kernels. Each kernel smooths the image in one direction (reducing noise) and computes the derivative in the perpendicular region (highlighting edges). Both operators use two kernels: one detects vertical edges, and one horizontal ones. After convolving the image with both kernels, the gradient magnitude and direction are computed.

$$\text{Magnitude} = \sqrt{G_x^2 + G_y^2} \qquad \text{Direction} = \arctan\left(\frac{G_y}{G_x}\right)$$

Prewitt is better for precise edge localization in cleaner images. Sobel is preferable in noisy images but may slightly blur edges.

2.3.1 Non-Maxima Suppression (NMS)

Detecting edges by gradient thresholding is inherently inaccurate, since **it's difficult to choose the right threshold** a priori. A better approach to detect edges may consist in finding the local maxima of the absolute value of the derivative of the signal.

When dealing with 2D images, we should look for:

- Maxima of the absolute value of the derivative (gradient magnitude).
- Along the gradient direction (orthogonal to the edge direction).

We don't know in advance the correct direction to carry out Non-Maxima Suppression (NMS). The direction has to be estimated locally based on the gradient's direction. The magnitude of the gradient has to be estimated at points which do not belong to the discrete pixel grid. Such values can be estimated by linear interpolation of those computed at the closest point belonging to the grid.

A final thresholding step on the magnitude of the gradient at the points selected by the NMS process typically helps pruning out unwanted edges due to either noise or less important details.

2.3.2 Canny's edge detector

Canny proposed to set forth quantitative criteria to measure the performance of an edge detector and then to find the optimal filter with respect to such criteria. The three criteria he proposed were:

- **Good detection**: correctly extract edges in noisy images.
- **Good localization**: distance between found and true edge should be minimum.
- **One response to one edge**: detect one single edge pixel at each true edge.

A straightforward Canny edge detector can be achieved by:

- Gaussian smoothing.
- Gradient computation.
- NMS along the gradient direction.

2D convolution by a Gaussian can be slow, so we can leverage on separability of the Gaussian function to speedup the calculation: $G(x, y) = G(x)G(y)$.

Non Maxima-Suppression (NMS) is often followed by thresholding of gradient magnitude to help distinguish between true "semantic" edges and unwanted ones. Edge **streaking** may occur when magnitude varies along object contours.

Canny proposed a "hysteresis" thresholding approach relying on a higher T_h and a lower T_l threshold. A pixel is taken as an edge if either the gradient magnitude is higher than T_h or higher than T_l and the pixel is a neighbor of an already detected edge.

The hysteresis thresholding is usually carried out by tracking edge pixels along contours. First the edge candidates are provided by NMS, then all strong edges are picked, and then for each strong edge we track the weak edges along contours.

Zero-crossing Instead of maximum values we can look for zero-crossing of the second derivative of the signal to locate edges (instead of the peaks of the first derivative). This requires significant computational effort since we are calculating second derivatives.

2.3.3 Second derivative along the gradient & Laplacian

The second derivative along the gradient's direction can be obtained as $n^T H n$.

- **Unit vector along the gradient's direction** $n = \frac{\nabla I(x,y)}{||\nabla I(x,y)||}$
- **Hessian matrix** $H = \begin{bmatrix} \frac{\partial^2 I(x,y)}{\partial x^2} & \frac{\partial^2 I(x,y)}{\partial x \partial y} \\ \frac{\partial^2 I(x,y)}{\partial y \partial x} & \frac{\partial^2 I(x,y)}{\partial x^2} \end{bmatrix}$

Computing the second derivative along the gradient turns out very expensive.

Discrete Laplacian We can use the forward and backward differences to approximate first and second order derivatives. It can be shown that the zero-crossing of the Laplacian typically lay close to those of the second derivative along the gradient. Yet, the former differential operator is much faster to compute.

2.3.4 Laplacian of Gaussian (LoG)

A robust edge detector should include a smoothing step to filter out noise. Edge detection by using the Laplacian of Gaussian (LoG) can be summarized as follows:

- **Gaussian smoothing**: $\tilde{I}(x, y) = I(x, y) * G(x, y)$.
- **Second order differentiation** by the Laplacian.
- Extraction of the **zero-crossing** of $\nabla^2 \tilde{I}(x, y)$

Practical implementations of the LoG may deploy the properties of convolutions to speed-up the computation.

We can find sign changes from minus to plus (and viceversa) between two consecutive pixels. Once a sign change is found, the actual edge may be localized:

- At the pixel where the LoG is positive (darker side of the edge)
- At the pixel where the LoG is negative (brighter side of the edge)
- At the pixel where the **absolute** value of the LoG is smaller (it's the best choice, since the edge turns out closer to the true zero-crossing).

Using a **higher σ yields less details**, so usually we use it for noisy images.

2.4 Feature detection and matching

Feature detection is useful for object detection, since we can look for features in the source image and try to find them again in the target image. Several computer vision tasks deal with finding "Corresponding Points" between two (or more) images of a scene. Correspondences are image points which are the projection of the same 3D point in different views of the scene. Establishing correspondences may be difficult, as the points may look different in different views.

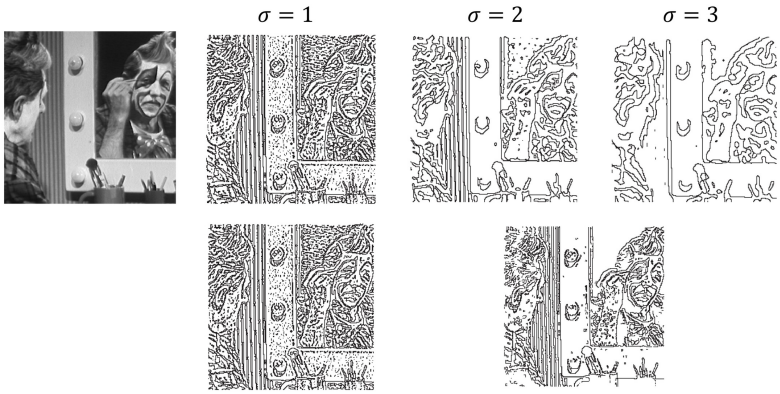

Figure 20: Examples of LoG application

2.4.1 Local invariant features paradigm

The task of establishing correspondences is split into 3 successive steps:

- **Detection** of salient points.
- Computation of a **suitable descriptor** based on pixels in the keypoint neighbourhood.
- **Matching** descriptors between images.

Descriptors should be **invariant** to as many transformations as possible. Ideally we want scale/rotation/illumination invariance.

2.4.2 Properties of good detectors/descriptors

- Detector:
  - Repeatability: it should find the same keypoints in different views of the scene despite the transformations.
  - Saliency: it should find keypoints surrounded by informative patterns.
- Descriptor:
  - Distinctiveness vs. robustness trade-off: the algorithm should capture the salient information around a keypoint.
  - Compactness: the description should be as concise as possible.

Speed is desirable for both, and in particular for detectors, which need to be run on the whole image (while descriptors are computed at keypoints only).

Edge pixels can be hardly told apart as they look very similar along the direction perpendicular to the gradient. Edges are locally ambiguous, since there are many other points that look just the same.

2.4.3 Moravec Interest Point Detector

We can define the **cornerness** at a point p, which is given by the minimum squared difference between the patch centered at p and those centered at its 8 neighbours:

$$C(p) = \min_{q \in n_8(p)} ||N(p) - N(q)||^2$$

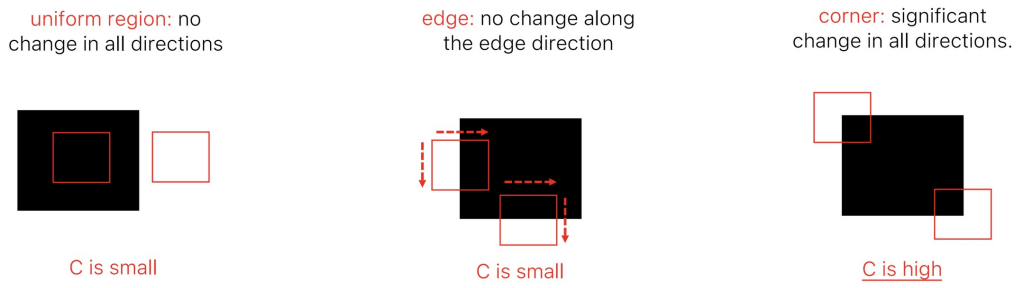

Figure 21: Cornerness of an image segment

After computing the cornerness we threshold and do Non-Maxima Suppression.

2.4.4 Harris Corner Detector

Harris & Stephens proposed to rely on a continuous formulation of the Moravec's "error" function. Assume to shift the image with a generic infinitesimal shift $(\Delta x, \Delta y)$: $w(x, y)$ is a window set to 1 around the pixel under evaluation and 0 in all the image. In the end we consider only the pixel around the (x, y) position.

Due to the shift being infinitesimal, we can deploy Taylor's expansion of the intensity function at (x, y) : $f(x + \Delta x) = f(x) + f'(x)\Delta x$

M encodes the local image structure around the considered pixel. We hypothesize that M is a diagonal matrix $M = \begin{bmatrix} \sum_{x,y} w(x,y) I_x(x,y)^2 & \sum_{x,y} w(x,y) I_x(x,y) I_y(x,y) \\ \sum_{x,y} w(x,y) I_y(x,y) I_x(x,y) & \sum_{x,y} w(x,y) I_y(x,y)^2 \end{bmatrix} = \begin{bmatrix} \lambda_1 & 0 \\ 0 & \lambda_2 \end{bmatrix}$

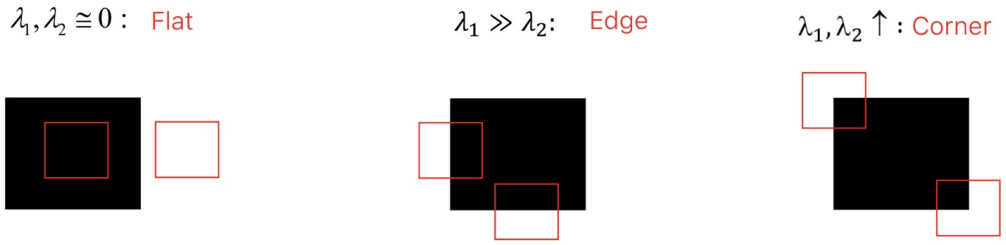

Figure 22: Harris corner detector and lambda values

The previous considerations have general validity as M is real and symmatric, and thus can always be diagonalized by a rotation of the image coordinate system.

$$M = R \begin{bmatrix} \lambda_1 & 0 \\ 0 & \lambda_2 \end{bmatrix} R^T$$

The columns of R are the orthogonal unit eigenvectors of M. λ_i are the corresponding eigenvalues. R^T is the rotation matrix that aligns the image axes to the eigenvectors of M.

Computing eigenvalues at each pixel is costly, so we can compute a more efficient "cornerness" function that gives a result C that is positive on a corner, negative on an edge an about 0 on a flat surface.

The **Harris corner detection algorithm** can thus be summarized as follows:

1. Compute C at each pixel.
2. Select all pixels where C is higher than a chosen positive threshold T.
3. Within the previous set, detect as corners only those pixels that are local maxima of C (NMS).

Eigenvalues of M are invariant to a rotation of the image axes, and thus so is Harris cornerness function. It also invariant to additive intensity changes. However, it's not invariant to scale changes, as corner structures may degrade or transform into edges under significant scaling, nor to multiplicative intensity variations which scale gradients and alter the corner response magnitude unless thresholds are adaptively adjusted.

2.4.5 Scale-Space

Scale invariance is the main issue adressed by second generation local invariant features. The key idea is to apply a fixed-size detection tools on increasingly down-sampled and smoothed versions of the input image.

As we move along scales, small details should continuously disappear and no structure should be introduced.

A Scale-Space is a **one-parameter family of images** created from the original one so that the structures at smaller scales are successively suppressed by smoothing operations.

A Scale-Space must be realized by Gaussian Smoothing: $L(x, y, \sigma) = G(x, y, \sigma) * I(x, y)$. A Scale-Space is created by repeatedly smoothing the original image with larger and larger Gaussian kernels.

Figure 23: We increase the blur as we reduce the image size

Feature Detection & Scale Selection As features exist across a range of scales how do we establish at which scale a feature turns out maximally interesting and should therefore be described?

As we filter more by using a higher sigma, derivatives tends to become weaker. To compensate, Lindeberg proposed to multiply/normalize derivatives by sigma (doing scale-normalization).

Scale-Normalized LoG The scale-normalized Laplacian Of Gaussian (LoG) is:

$$F(x, y, \sigma) = \sigma^2 \nabla^2 L(x, y, \sigma) = \sigma^2 (\nabla^2 G(x, y, \sigma) * I(x, y))$$

where σ^2 is the normalization factor.

The **scale-normalized LoG detects blobs** (regions with intensity variations) by combining Gaussian Smoothing (which reduces noise and suppresses fine details) and Laplacian Operator (which highlights regions of rapid intensity change).

Scale normalization is introduced since the raw LoG response diminishes as the scale (σ) increases, biasing detection toward smaller blobs.

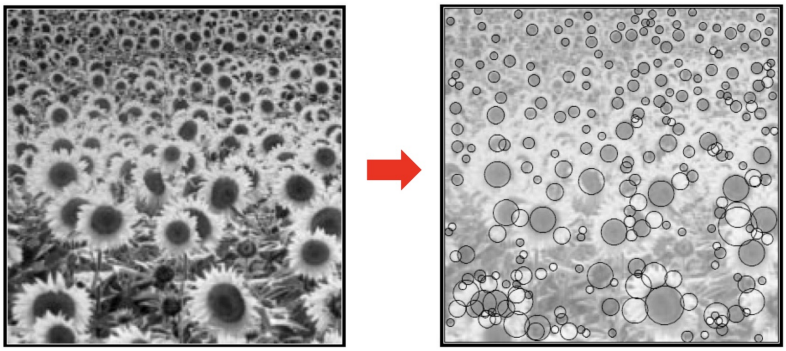

Figure 24: LoG filter locates blobs

Difference of Gaussian (DoG) Lowe proposed to detect keypoints by seeking for the extrema of the DoG (Difference of Gaussian) function across the (x, y, σ) domain.

$$DoG(x, y, \sigma) = (G(x, y, k\sigma) - G(x, y, \sigma)) * I(x, y) = L(x, y, k\sigma) - L(x, y, \sigma)$$

This approach provides a computationally efficient approximation of Lindeberg's scale-normalized LoG.

$$G(x, y, k\sigma) - G(x, y, \sigma) \approx (k - 1)\sigma^2 \nabla^2 G(x, y, \sigma) * I(x, y)$$

Both detectors are rotation invariant and find blob-like features.

In the DoG we compute several Gaussian smoothed functions within an octave. For each pair we take the differences, then we seek for extrema in the DoG.

Extrema detection A point (x, y, σ) is detected as a keypoint if and only if its DoG is higher (or lower) than that of the 26 neighbour (8 at the same scale and $18 = 9 + 9$ at the two nearby scales) in the (x, y, σ) space.

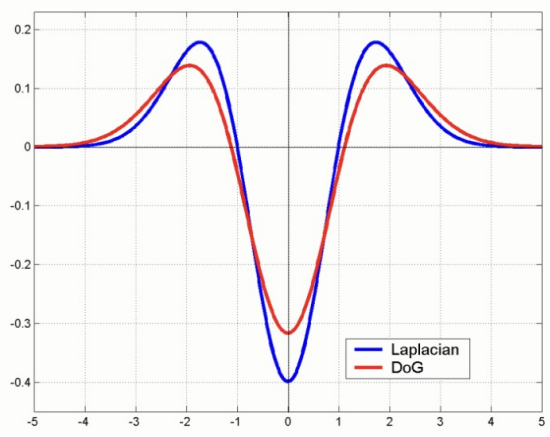

Figure 25: Lowe proves that this is a scaled version of Lindeberg

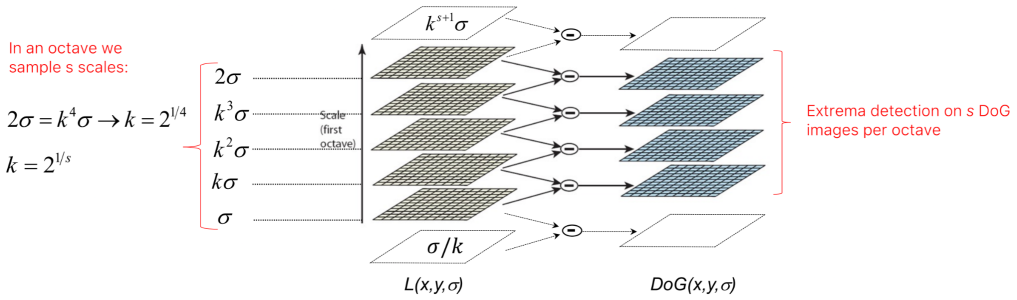

Figure 26: Difference of Gaussian

According to the original article the best number of sclaes within an octave is $s = 3$, initial σ for each octave should be $\sigma = 1.6$ and the input image is enlarged by a factor of 2 in both dimensions.

After detecting points as local extrema, the next step is to prune weak and unstable responses to ensure robustness. Keypoints with low contrast, corresponding to weak DoG responses, are often sensitive to noise and less repeatable across different images.

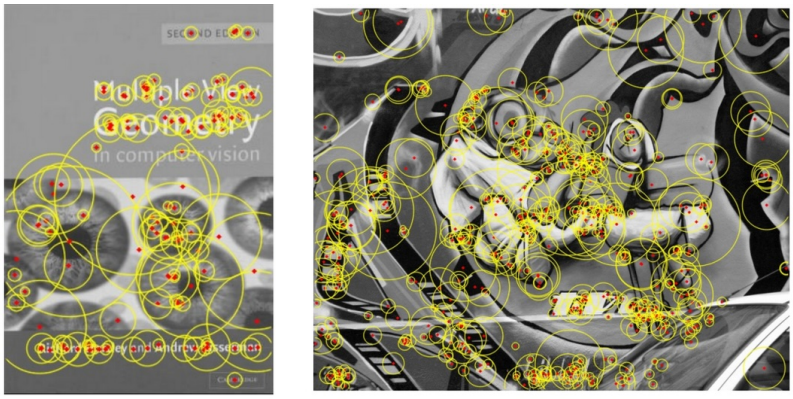

Figure 27: The size of the circle is proportional to the scale of the feature (σ)

2.4.6 Scale and Rotation Invariance Description

DoG are **rotation invariant because of circular simmetry**. Once each keypoint has been extracted, a surrounding patch is considered to compute its descriptor (scale and rotation invariant).

We need to identify a **prominent direction** inherent to the patch (the canonical orientation) and, based on such direction, define a local reference frame. A reasonable choice consists in identifying the **direction along which most of the gradient is found**.

To compute the canoncial orientation we need to define a scale and rotation invariant descrip-

tion. Once each keypoint has been extracted, a surrounding patch is considered to compute its descriptor (scale and rotation invariant).

- Scale invariance: the patch is taken from the stack of images that correspond to the characteristic scale.
- Rotation invariance: a canonical patch orientation is computed, so that the descriptor can then be computed on a canonically-oriented patch (orientation with respect to a new reference system, not the one of the image).

Lowe proposed to compute the **canoncial orientation of DoG keypoints** as follows: given the keypoint, the magnitude and orientation of the gradient are computed at each pixel of the associated Gaussian-smoothed image, L:

- $m(x,y) = \sqrt{(L(x+1,y) - L(x-1,y))^2 + (L(x,y+1) - L(x,y-1))^2}$
- $\theta(x,y) = \tan^{-1} \frac{L(x,y+1)-L(x,y-1)}{L(x+1,y)-L(x-1,y)}$

We can then compute an **orientation histogram** by accumulating the contributions of the pixels belongigng to a neighborhood of the keypoint location (a bin size of 10 deg). The characteristic orientation of the keypoint is given by the highest peak of the orientation histogram. Other peaks higher than 80% of the main one would be kept as well. A keypoint may have multiple canonical orientations and, in turn, multiple descriptors sharing the same location/scale with diverse orientations (this happen rarely, about on 15% of the keypoints).

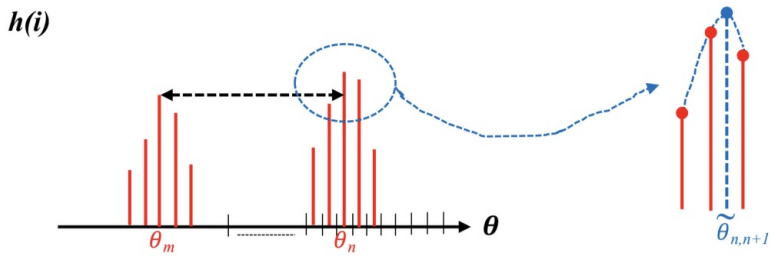

Figure 28: This is an ambiguous keypoint, we have two prominent decisions

2.4.7 SIFT Descriptor

The **SIFT (Scale Invariant Feature Transform)** descriptor is computed as follows:

- 16×16 oriented pixel grid around each keypoint is considered.
- This is further divided into 4×4 regions (each of size 4×4 pixels).
- A gradient orientation histogram is created for each region.
- Each histogram has 8 bins.
- Each pixel in the region contributes to its designated bin according to gradient magnitude and gaussian weighting function centered at the keypoint (with σ equal to half the grid size).

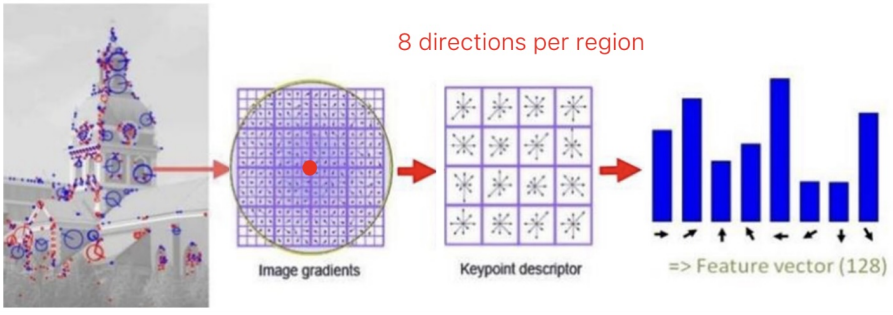

Figure 29: The descriptor size is given by the number of regions times the number of histogram bins per region

Matching process The descriptor is normalized to unit length to gain invariance with respect to affine intensity changes. Descriptors like SIFT are compared across diverse views of a scene to find corresponding keypoints. This is a classical Nearest Neighbour (NN) seach problem. Given a set S of points, p_i, in a matric space M and a query point $q \in M$, find the p, closest to q. We

wish to match the local features computed from an image under analysis (target image T) to those already computed from a reference image (R) or a set of reference images.

For each feature in T we look for the most similar one in R:

- The features in T represent the query points, q.
- The features in R provide set S.
- When matching SIFT descriptors the distance typically used is the Euclidean distance.

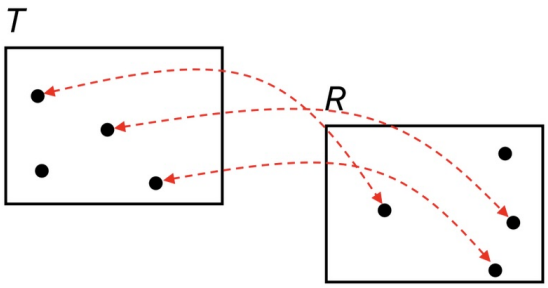

Figure 30: Image matching process with SIFT

The found Nearest Neighbour (NN) does not necessarily provide a valid correspondence as some features in T may not have a corresponding feature in R. We enforce a criteria to accept/reject a match found by the NN search process. The simplest thing to do is to use a threshold. Lowe showed that $T = 0.8$ may allow for rejecting 90% of the wrong matches while missing only 5% of those correct.

Exhaustively searching for the NN of the query feature, q, has linear complexity in the size of S. This is slow, so efficient indexing techniques are exploited to speed-up the NN-search process. The main indexing technique exploited for feature matching is known as k-d tree.

2.5 Camera Calibration

Camera Calibration is important for taking quantitative measurements from images. In the **perspective projection** model, given a point in the 3D space $M = [x, y, z]^T$, with coordinates given in the Camera Reference Frame (CRF). Its projection onto the image plane I is denoted as $m = [u, v]^T$.

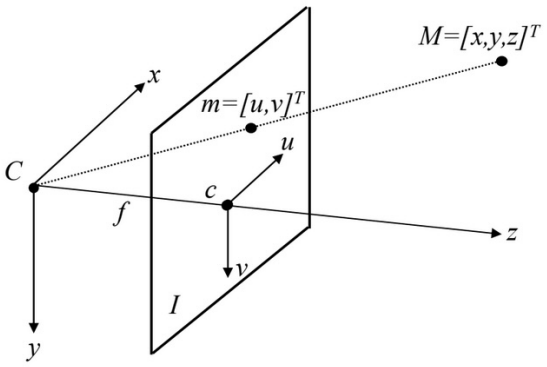

Figure 31: Perspective Projection Model (PPM)

2.5.1 Projective Space

The **Physical Space** is a 3D Euclidean Space ($\mathbb{R}^3$) whose points can be represented as 3D vectors in a given reference frame. In this space parallel lines do not intersect. Points at infinity cannot be represented in this vector space.

The **Projective Space** is a mathematical engine to handle the geometry of image formations. In the Projective space we append one more coordinate to the Euclidean triplets. A point is represented by an equivalence class of quadruples, wherein equivalent quadruples differ just by a multiplicative factor. This is called the **homogeneous coordinates** representation of the 3D point

having Euclidean coordinates (x, y, z). The space associated with the homogeneous coordinate's representation is called Projective Space, denoted as P^3

We are interested in Projective Spaces because Perspective Projection is **more conveniently** dealt with using projective coordinates.

The point at infinity is a point in the space, the vanishing point is a point into the image plane. Points at infinity of the 3D lines are the points of the 3D Projective Space **having the fourth coordinate equal to 0**.

To map such points into the Euclidean Space we would divide by the fourth coordinate (which is 0) which is not a valid representation in the Euclidean Space.

The point $(0, 0, 0, 0)$ it's not the origin, but an undefined point. The origin is represented in homogeneous coordinates as $(0, 0, 0, k)$, with $k \neq 0$.

Given a 3D point $\tilde{M} = [x, y, z]^T$ (with coordinates expressed in the Camera Reference Frame) and its 2D projection onto the image plane $\tilde{m} = [u, v]^T$.

In homogeneous coordinates the perspective projection becomes a linear transformation.

$$\begin{bmatrix} u \\ v \\ 1 \end{bmatrix} = \begin{bmatrix} f & 0 & 0 & 0 \\ 0 & f & 0 & 0 \\ 0 & 0 & 1 & 0 \end{bmatrix} \begin{bmatrix} x \\ y \\ z \\ 1 \end{bmatrix}$$

Which in matrix notation is $\tilde{m} \approx \tilde{P}\tilde{M}$, where $\approx$ means "equal up to an arbitrary scale factor". $\tilde{P}$ represents the geometric camera model, and is known as **Perspective Projection Matrix (PPM)**. The operation carried out by the PPM is that of scaling lateral coordinates according to the distance from the camera (z). The actual focal length just introduces an additional scaling factor of projected coordinates.

The is just an abstraction, which is quite convenient but also useless, since there is no way to measure world coordinates in a reference frame which is basically an abstraction of a camera.

2.5.2 A more comprehensive camera model

To come up with a really useful camera model we need to take in account two additional issues:

- Image digitization.
- The 6 DOF rigid motion between the Camera Reference Frame (CRF) and the World Reference Frame (WRF).

Digitization can be accounted for by including into the projection equations the scaling factors along the two axis due to the quantization associated with the horizontal and vertical pixel size, this is because we have a discrete grid of pixels.

We also need to model the translation of the piercing point (intersection between the optical axis and the image plane) with respect to the origin of the image coordinate system. This is needed to move the reference frame from the center of the CMOS in the camera to the top left corner, since we don't want to use negative coordinates.

2.5.3 Intrinsic Parameter Matrix

Now the Perspective Projection Matrix can be written as:

$$\tilde{P} = \begin{bmatrix} fk_u & 0 & u_0 & 0 \\ 0 & fk_v & v_0 & 0 \\ 0 & 0 & 1 & 0 \end{bmatrix} = \begin{bmatrix} fk_u & 0 & u_0 \\ 0 & fk_v & v_0 \\ 0 & 0 & 1 \end{bmatrix} \begin{bmatrix} 1 & 0 & 0 & 0 \\ 0 & 1 & 0 & 0 \\ 0 & 0 & 1 & 0 \end{bmatrix} = A[I|0]$$

Matrix A, models the characteristics of the image sensing device and is called **Intrinstic Parameter Matrix** The smallest number of intrinsic parameters is thus 4. The intrinstic parameter matrix contains infromation about: focal length, pixel dimension and camera center.

2.5.4 Rigid motion between CRF and WRF

We need to apply a roto-translation to relate the World Reference Frame to the Camera Reference Frame. The relation between the coordinates of a point in the two reference frames is:

$$W = \begin{bmatrix} X \\ Y \\ Z \\ 1 \end{bmatrix}, M = \begin{bmatrix} x \\ y \\ z \\ 1 \end{bmatrix} \Rightarrow M = \begin{bmatrix} R & T \\ 0 & 1 \end{bmatrix} W = GW$$

To map a 3D point expressed in the Camera Reference Frame: $k\tilde{m} = A[I|0]\tilde{M}$

The general from of the Perspective Projection Matrix can be expressed as follows: $\tilde{P} = A[I|0]G$ or also $\tilde{P} = A[R|T]$.

Extrinsic Parameters G is called **Extrinsic Parameter Matrix** and it encodes the position and orientation of the camera with respect to the World Reference Frame. The rotation matrix has only 3 independent parameters, which correspond to the rotation angles around the axis of the reference frame. T has 3 independent parameters. The total number of **extrinsic parameters** is 6 (3 translation, 3 rotation). A has 4 independent parameters. The general form of the Perspective Projection Matrix can be thought of as encoding:

- the position of the camera with respect to the world into G.
- the actual characteristics of the sensing device into A.

2.5.5 P as a Homography

We just need the relation between the camera and the plane, then we can measure everything on that plane.

If the camera is imaging a planar scene, we can assume the z-axis of the World Reference Frame to be perpendicular to the plane such that all 3D points will have their z-coordinate equal to 0. The Perspective Projection Matrix then becomes a simpler transformation defined by a $3x3$ matrix.

$$k\tilde{m} = \tilde{P}\tilde{w} \begin{bmatrix} p_{1,1} & p_{1,2} & \cancel{p_{1,3}} & p_{1,4} \\ p_{2,1} & p_{2,2} & \cancel{p_{2,3}} & p_{2,4} \\ p_{3,1} & p_{3,2} & \cancel{p_{3,3}} & p_{3,4} \end{bmatrix} \begin{bmatrix} x \\ y \\ 0 \\ 1 \end{bmatrix} = \begin{bmatrix} p_{1,1} & p_{1,2} & p_{1,4} \\ p_{2,1} & p_{2,2} & p_{2,4} \\ p_{3,1} & p_{3,2} & p_{3,4} \end{bmatrix} \begin{bmatrix} x \\ y \\ 1 \end{bmatrix} = H\tilde{M}$$

Such a transformation, denoted here as H, is known as **homography** and represents a general linear transformation between projective planes. A homography is then a projective transformation between two planes or a mapping between two planar projection of an image.

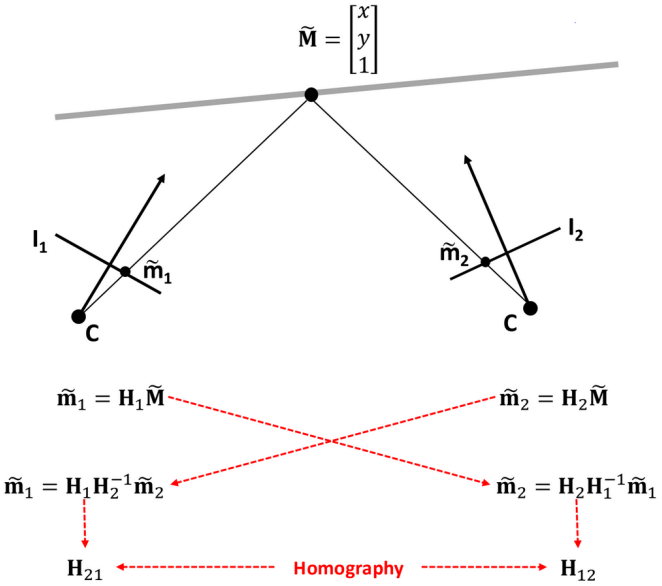

Figure 32: Any two images of a planar scene are related by a homography

2.5.6 Lens distortion

The Perspective Projection Matrix is based on the pinhole camera model, however, real lenses introduce distortions with respect to the pure pinhole model. We also have lens distortion, which

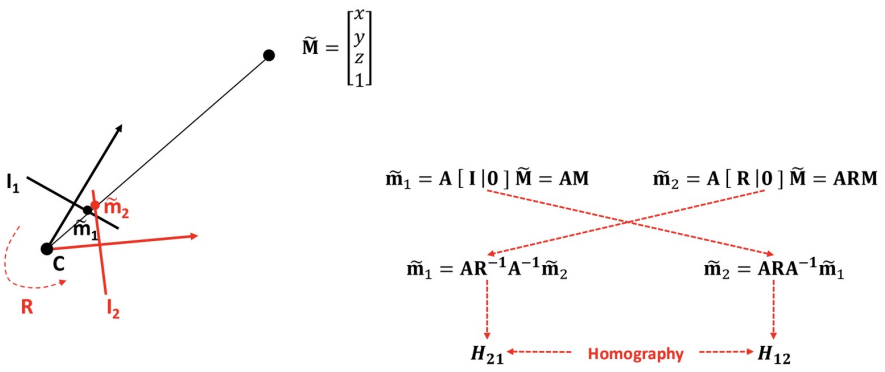

Figure 33: Any two images taken by a camera rotating about the optical center are related by a homography

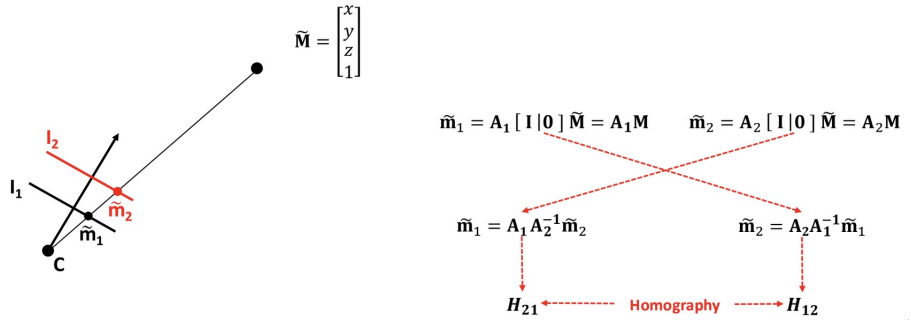

Figure 34: Any two images taken by different cameras in fexed pose are related bu a homography

is modelled through additional parameters that don't alter the form of the Perspective Projection Matrix.

We have two types of lens distortion: barrel distortion which bends straight lines outwards, and pincushion distortion, which causes straight lines to curve inward.

2.5.7 Calibration

We now have the Perspective Projection Matrix camera model, which can be decomposed in:

- Intrinsic parameter matrix A.
- Rotation matrix R.
- Translation vector T.

Camera calibration is the process whereby **all parameters defining the camera model are estimated** for a specific camera device. Depending on the application, **either the Perspective Projection Matrix (PMM) only, or also its independent components** (A,R,T) need to be estimated.

There are many camera calibration algorithms, but the basic process always relies on setting up a linear system of equations given a set of known 3D-2D correspondences. To obtain the correspondences we use calibration targets, which have easily detectable features.

The approaches can be split into:

- Those relying on a single image containing a known pattern.
- Those relying on several different images of one given planar pattern.

2.5.8 Zhang's method for Camera Calibration

We use a chessboard pattern of which we know the number of internal corners and the size of the squares. Internal corners can be easily detected by standard algorithms, like the Harris corner detector. Typically the camera is fixed and you move the calibration target in front of the camera. The $[RT]$ are estimated with respect to the reference system attached to the target, but it changes alongside with the pattern. In each image the 3D world reference frame is taken at the top-left corner of the pattern. Each image requires its own estimate of the extrinstic parameters, as they are different from one to the other. Due to the choice of the world reference frame associated with calibration images, in each of them we consider only 3D points with $z = 0$. The Perspective

Projection Matrix boils down to a simpler transformation defined by an homography 3×3 matrix, like with P as a homography.

$$k\tilde{m} = \tilde{P}\tilde{w} \begin{bmatrix} p_{1,1} & p_{1,2} & \cancel{p_{1,3}} & p_{1,4} \\ p_{2,1} & p_{2,2} & \cancel{p_{2,3}} & p_{2,4} \\ p_{3,1} & p_{3,2} & \cancel{p_{3,3}} & p_{3,4} \end{bmatrix} \begin{bmatrix} x \\ y \\ \cancel{0} \\ 1 \end{bmatrix} = \begin{bmatrix} p_{1,1} & p_{1,2} & p_{1,4} \\ p_{2,1} & p_{2,2} & p_{2,4} \\ p_{3,1} & p_{3,2} & p_{3,4} \end{bmatrix} \begin{bmatrix} x \\ y \\ 1 \end{bmatrix} = H\tilde{M}$$

Given a pattern with m corners, we can write m systems of 3 linear equations, where:

- Both 3D as well as 2D coordinates are known due to the corners having been detected in the i-th image and the unknowns are thus the 9 elements in H_i.
- H_i (and P_i alike) is known up to an arbitrary scale factor, the independent elements in H_i are 8.

There are plenty of methods for the estimation
The Zhang's method can be summarized as:

1. Acquire n images of a planar pattern with m internal corners.
2. For each image compute an initial guess for homography H_i.
3. Refine eaech H_i by minimizing the reprojection error.
4. Get an initial guess for A given the homographies H_i.
5. Given A and H_i, get an initial guess for R_i and T_i.
6. Compute an initial guess for lens distortion parameters k.
7. Refine all parameters A, R_i, T_i, k by minimizing the reprojection error.

2.5.9 Image warping

After applying the warping function you get real coordinates not discrete ones. During the mapping, some pixels of the destination image may be not rounded perfectly. What if more pixels go to the same position?

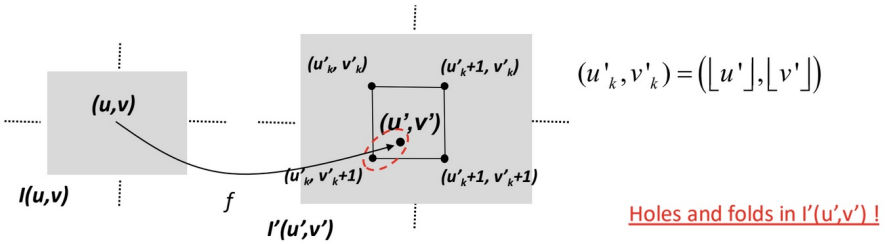

Figure 35: A better choice consists in mapping to the closest point into the destination image

Since the coordinates are always real values the different mapping strategies can be to map the closest point or to interpolate between the 4 closest points.

3 Advanced Topics in Deep Learning for Computer Vision

3.1 Recall on CNNs

In representation learning we try to find good ways of representing data, often by learning a useful transformation of the raw data. Deep learning is a subset of representation learning.

3.1.1 Gradient descent

Neural networks are usually trained using iterative, gradient-based optimizers that drive the cost function to a very low value. The convergence point of gradient descent depends on the initial values of the parameters. For feedforward neural networks it's important to initialize all weights to small random values and to initialize biases to zero or to small positive values. To apply gradient based learning we must choose a cost function and how to represent the output of the model. The derivative $f'(x)$ gives the slope of $f(x)$ at the point x. The derivative is useful for minimizing a function because it tells us how to change x in order to make a small improvement in y. A point that obtains the absolute lowest value of $f(x)$ is a global minimum.

To reach the minimum we use the formula $w' = w - \alpha\frac{\partial J(w,b)}{\partial w}$ $b' = b - \alpha\frac{\partial J(w,b)}{\partial b}$, where α is the learning rate, which controls how big are the steps that we take during the gradient descent. If the slope is positive, we subtract the quantity in order to reach the minimum, or else we do the opposite thing.

As the training set size grows to billions of examples, the time to take a single gradient step becomes prohibitively long. Stochastic/Minibatch gradient descent are extensions of the gradient descent algorithm. We can sample a minibatch of examples drawn uniformly from the training set (1 for stochastic). It's like training every time on a different (smaller) training set.

Optimizers: momentum Momentum was designed to accelerate learning, especially in the face of high curvature, small but consistent gradients, or noisy gradients. The size of the step depends on how large and how aligned a sequence of gradients are. The step size is largest when many successive gradients point in the same direction. Momentum smooths the step of the gradient descent in its path to the minimum. We compute: $W^{[l+1]} = W^{[l]} - \alpha v_{W^{[l+1]}}$, where $v_{W^{[l+1]}} = \beta v_{W^{[l]}} + (1-\beta)\frac{\partial J(...)}{\partial W^{[l]}}$. Root Mean Square Propagation (RMSprop) uses an exponentially decaying average to discard history from the extreme past so that it doesn't impede the convergence.

Optimizers: Adam The name derives from "adaptive moments", and it can be seen as the combination of RMSprop and momentum. It's fairly robust to the choice of hyperparameters, though the learning rate sometimes needs to be changed from the suggested default. There is a first order and a seond order Adam. The first order Adam uses the gradient and its moving averages (first moments) to update the parameters. The second order Adam incorporates information about the curvature of the loss surface, using approximations of the Hessian or second order derivatives, which leads to more informed and potentially more efficient updates but requires more computational resources.

3.1.2 Convolutions and filters

An image is characterized by height, width and number of channels.

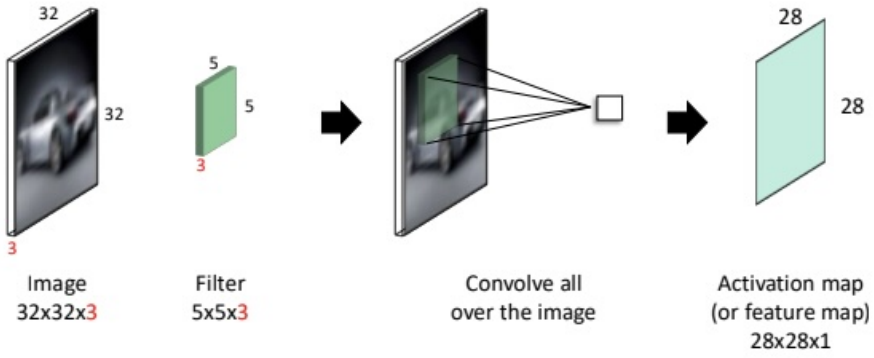

Figure 36: A convolutional filter has the **same depth** of the input volume, so the output dimension is 1.

We can also train more than one filer, where each filter outputs a feature map. By stacking activation maps we get a new volume.

Since convolutions shrink the images we can use padding to preserve the edges. We have always considered a stride of 1 (moving the convolutional filter by one pixel), but we can also use different stride sizes to shrink the image.

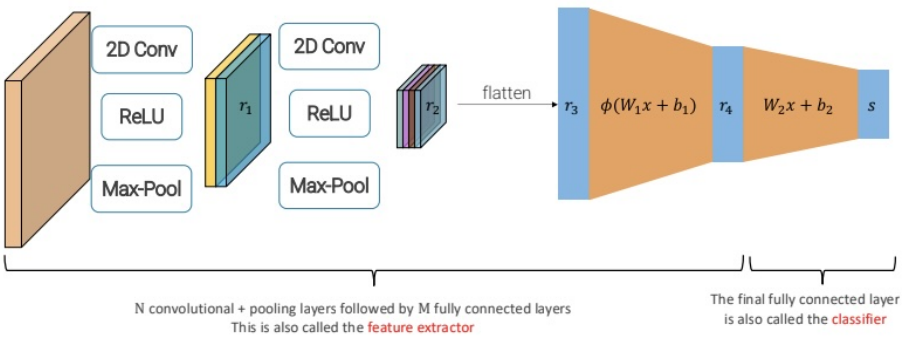

Figure 37: By stacking together convolutional filters, pooling layers and fully connected layers we can design a Deep CNN.

Pooling A pooling layer is used to reduce the size of the representation in order to speedup computation. Pooling comes usually after each conv layer or after a block (or set) of conv layers. It's applied to each activation map independently.

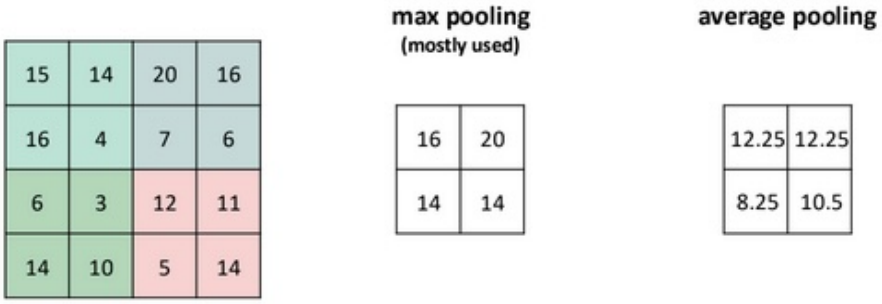

Figure 38: Example: pooling of dimension 2 and stride 2.

Receptive fields The input pixels affecting a hidden unit are called its receptive field. We can encode the information in all the pixels to a single point. We go from spatial to semantic information (we transform spatial information to semantic information).

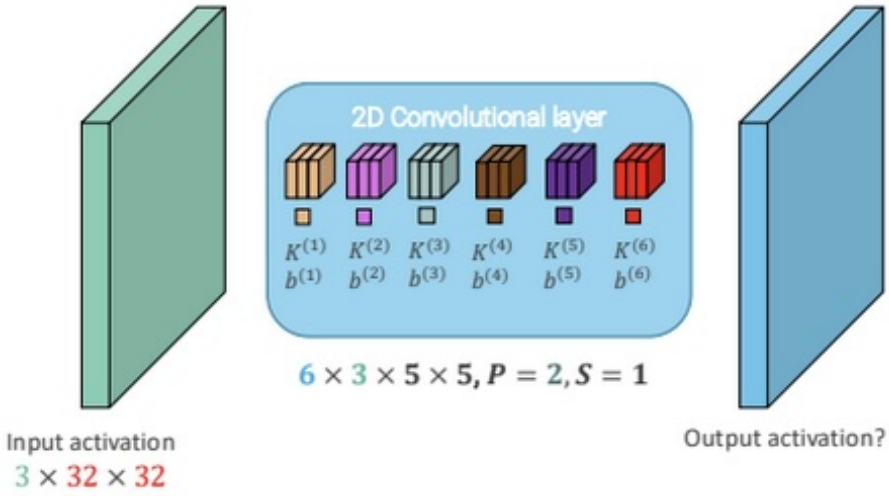

Figure 39:

Convolution parameters and flops As we can see in 39, the number of learnable parametes for the convolutional layer is $6 \times (3 \times 5 \times 5 + 1) = 6 \times 76 = 456$ (6 convolutional blocks, 3 channels per

convolutional block, 5×5 convolution,). The size of the output is $H_{\text{out}} = W_{\text{out}} = 32-5+2*2+1 = 32$. Hence, there are $6 \times 32 \times 32 = 6144$ values in the output activation ($\approxeq$ 24KB).

Since each of them is obtained as the dot product between the weights and the input, which requires to perform n multiplications and n summations for inputs of size n, i.e. $2n$ flops.

3.1.3 Batch Normalization (BatchNorm)

BatchNorm is a technique designed to stabilize and accelerate the training of deep neural networks by addressing internal covariate shift: the change in the distribution of layer activations caused by updates to preceding layers during training. By normalizing activations at each layer, BatchNorm ensures that gradients are propagated more effectively, enabling coordinated updates across deep networks.

Let $Z^{[l]}$ be a minibatch of activations of the l-th layer to be normalized. To normalize $Z^{[l]}$, we replace it with: $Z^{[l]}_{norm} = \frac{Z^{[l]}-\mu}{\sigma}$, where μ is a vector containing the mean of each unit and σ is a vector containing the mean of each unit and σ is a vector containing the standard deviation of each unit. μ and σ are running averages of the values seen during training. BatchNorm helps with speeding up the training, and has a slight regularization effect (but we don't use it for this reason).

We use LayerNorm for fully connected layers because it normalizes per sample, making it batch-size independent. We use InstanceNorm for convolutional layers because it normalizes per sample and per channel.

3.1.4 Dropout regularization

Dropout randomly deactivates a fraction of neurons during training, effectively training an ensemble of smaller sub-networks. For each layer, you set a dropout probability, determining the chance a neuron is ignored in a forward pass. This helps to prevent overfitting because we don't associate a certain pattern to a certain output of the network.

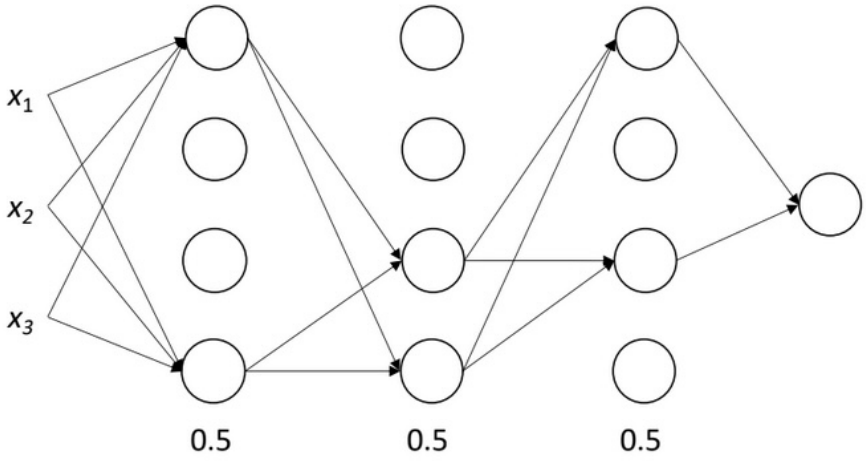

Figure 40: Each layer has a 50% dropout probability

Dropout and normalization are used only at training time. When we test the network we switch off dropout and regularization.

Another powerful regularization technique is just having more data.

3.1.5 Data augmentation

We can create more data by modifying the images we already have. We must only make transformations which keep the labels valid. We can, for example, sample random crops/scales of the data or do color augmentation.

Cutout is the process where we remove a random square region of the input image. This forces the network to use a more diverse set of features, helping generalization. It's gray because we subtract the mean from this pictures, and so the number in the cutout becomes 0.

3.2 CNNs

3.2.1 AlexNet & ZFnet

In 2012 Alex Krizhevsky proposed AlexNet, which had almost a 9% of improvement on SOTA.

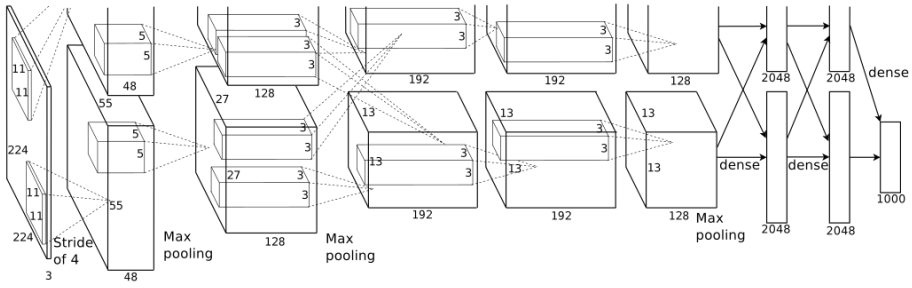

Figure 41: AlexNet architecture

In the image 41, we see only one half of the network, since the architecture is replicated identically 2 times to be used on a 2 GPU setup. The network is composed by a **stem layer** at the beginning, which is a convolution layer that performs a fast reduction in the spatial size of the activations, mainly to reduce memory and computational cost. The first layer has two 11×11 kernels, which extracts corners/edges/blobs.

To counteract these problems ZFnet used 7×7 convolutions with stride 2 in the first layer and 5×5 convolutions with stride 2 also in the second convolutional layer.

3.2.2 VGG

To avoid the vanishing gradient problem VGG used 3×3 convolutions only, and didn't use the stem layer. The network was shallower, and used only convolutions and pooling. At the end it used the same flattening and classification head.

Pre initialization with weights from shallower architectures was crucial to let the training progress, since batch normalization wasn't yet invented.

			VGG-16	VGG-19
ConvNet Configuration				
A	B	C	D	E
11 weight layers	13 weight layers	16 weight layers	16 weight layers	19 weight layers
input (224 × 224 RGB image)				
conv3-64	conv3-64 **conv3-64**	conv3-64 conv3-64	conv3-64 conv3-64	conv3-64 conv3-64
maxpool				
conv3-128	conv3-128 **conv3-128**	conv3-128 conv3-128	conv3-128 conv3-128	conv3-128 conv3-128
maxpool				
conv3-256 conv3-256	conv3-256 conv3-256	conv3-256 conv3-256 **conv1-256**	conv3-256 conv3-256 **conv3-256**	conv3-256 conv3-256 conv3-256 **conv3-256**
maxpool				
conv3-512 conv3-512	conv3-512 conv3-512	conv3-512 conv3-512 **conv1-512**	conv3-512 conv3-512 **conv3-512**	conv3-512 conv3-512 conv3-512 **conv3-512**
maxpool				
conv3-512 conv3-512	conv3-512 conv3-512	conv3-512 conv3-512 **conv1-512**	conv3-512 conv3-512 **conv3-512**	conv3-512 conv3-512 conv3-512 **conv3-512**
maxpool				
FC-4096				
FC-4096				
FC-1000				
soft-max				

Figure 42: VGG architecture

VGG introduces the idea of designing a network as repetition of stages, i.e. a fixed combination of layers that process activations at the same spatial resolution. In VGG we have 3 types of blocks:

- `conv-conv-pool`.
- `conv-conv-conv-pool`.
- `conv-conv-conv-conv-pool` (we can get a more complex convolution by combining 3×3 convolutions).

One stage has the same receptive field of larger convolutions but requires less parameters and computation, and introduces more non-linearities.

The disadvantage is that the memory for activation doubles.

convolutional layer	params	flops	ReLUs	number of activations
$C \times C \times 5 \times 5$, $S = 1$, $P = 2$	$25C^2 + C$	$50C^2W_{in}H_{in}$	1	$C \times W_{in} \times H_{in}$
2 stacked $C \times C \times 3 \times 3$, $S = 1$, $P = 1$	$18C^2 + 2C$	$10C^2W_{in}H_{in}$	2	$2 \times C \times W_{in} \times H_{in}$

VGG-16 is composed by 138M parameters ($2.3x$ AlexNet), mostly in fully connected layers. The computational cost is $\approx$ 4 Tflops, mainly due to convolutions, and the network uses about $\approx$ 16.5 GB of memory.

3.2.3 Inception v1 (GoogLeNet)

The main hallmark of this architecture is the improved utilization of the computing resources inside the network. This was achieved by a carefully crafted design that allows for increasing the depth and width of the network while keeping the computational budget constant.

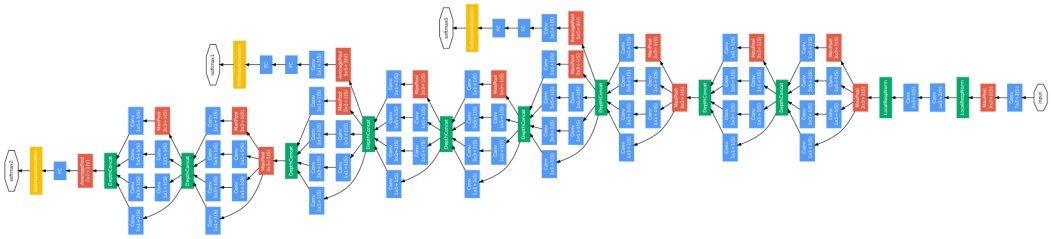

Figure 43: GoogLeNet architecture

The network is composed by stem layers which shrink the image size, a stack of inception modules where a combination of different operations are combined, and a final classifier. There are 22 trainable layers and about 100 modules (the blue and red blocks).

Stem layers Stem layers aggressively downsamples inputs: from 224 to 28 width/height in 5 layers. It brings it down a bit more gently than AlexNet. To reach 28×28, VGG uses 10 layers.

Naïve inception module The main idea of the inception module is that it consists of multiple pooling and convolution operations with different sizes (3×3, 5×5) in parallel, instead of using just one filter of a single size. However, there are two main problems:

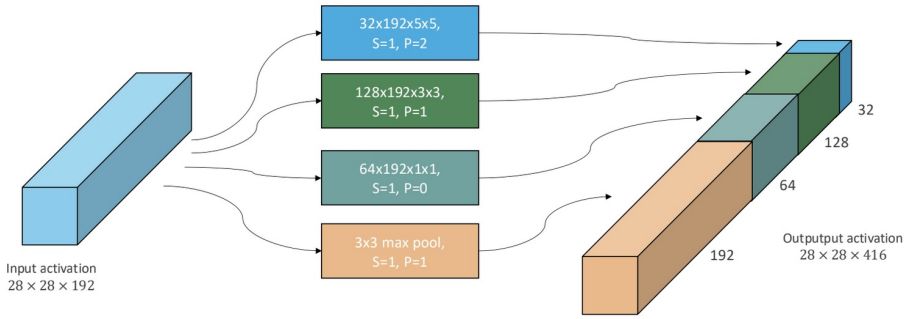

- Due to max-pool, the number of channels grows very fast when inception modules are stacked on top of each other.
- 5×5 and 3×3 convolutions on many channels become prohibitively expensive if we stack a lot of them.

1×1 convolutions and the inception module To overcome the problems, we use 1×1 convolutions before feeding the data into 3×3 or 5×5 convolutions. 1×1 convolutions don't reason locally, but along the channel on a single dimension. They allow us to change the depth of the activations while preserving the spatial size. This is effectively a dimensionality reduction.

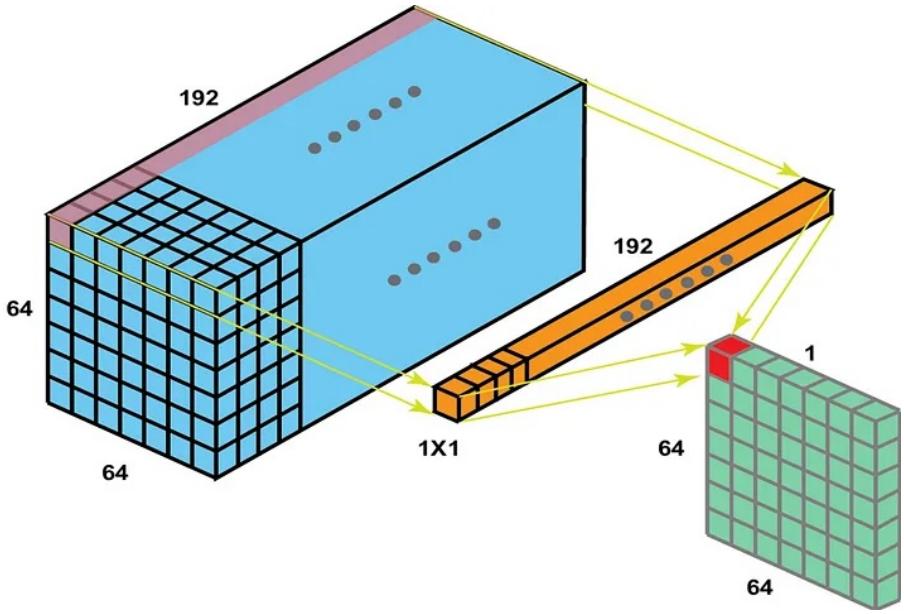

Figure 44: 1×1 convolution

By adding 1×1 convolutions before larger convs and after max pool we can:

- **Control the time complexity** of the larger convolutions by reducing the channel dimension.
- **Control the number of output channels** by reducing the depth of the max pool output.

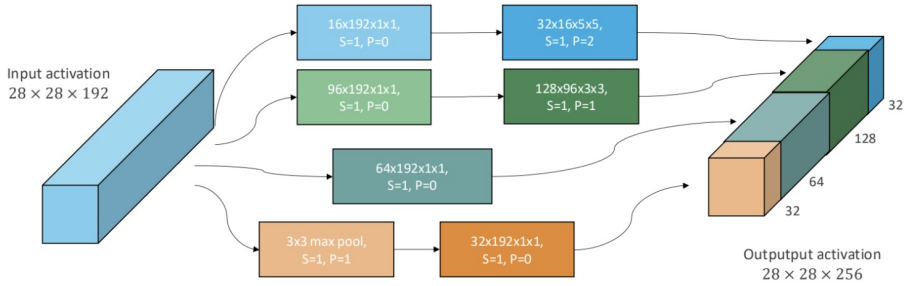

Fully-connected classifier vs global average pooling As we have seen the last 3 fully connected layers were the heaviest, since we had very high dimensional spatial information. To reduce the number of parameters needed between convolutional features and fully connected layers we get rid of spatial dimensions by averaging them out, because the activations should contain high level information.

3.2.4 Inception v3

Inception v3 leverages convolution factorizations to increase the computational efficiency and to reduce the number of parameters, the two main methods are:

- 3×3 followed by 3×3 instead of a 5×5 (VGG idea).
- 3×3 can be factorized in a 3×1 and 1×3.

3.2.5 Residual Networks (ResNet)

Optimizing very deep networks is hard. Residual blocks are implemented by adding skip connections which skip two convolutional layers.

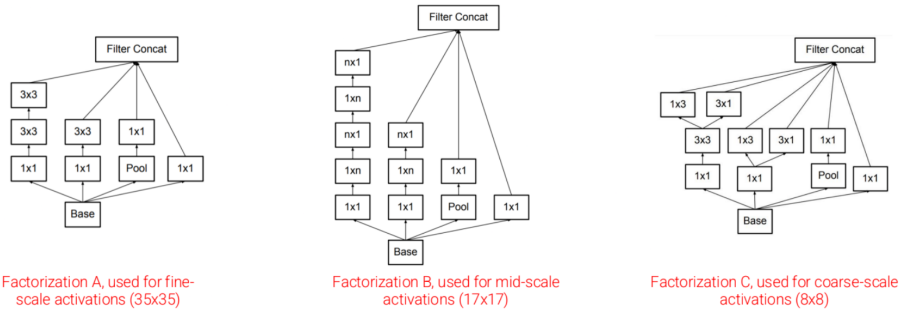

Figure 45: Instead of always using the same inception layers, we use inception with 3 different layers